PERGAMON

Computers in Biology and Medicine 30 (2000) 23–40

Computers in Biology and Medicine

www.elsevier.com/locate/compbiomed

Automated segmentation of multiple sclerosis lesions in multispectral MR imaging using fuzzy clustering

Abdel-Ouahab Boudraa[a,b,*], Sidi Mohammed Réda Dehak[b,c], Yue-Min Zhu[b], Chahin Pachai[b], Yong-Gang Bao[b], Jérôme Grimaud[d]

[a]*L2TI, Institut Galilée, Université Paris 13, Av. J.B. Clément, 93430, Villetanneuse, France*
[b]*CREATIS, CNRS UMR 5515, INSA 502, 69621, Villeurbanne, France*
[c]*ENST, Département Image, Rue Barrault, 75634, Paris, France*
[d]*Service de Neurologie, Hôpital d'Antiquaille, 69005, Lyon, France*

Received 30 March 1999; received in revised form 27 July 1999; accepted 27 August 1999

Abstract

A method is presented for fully automated detection of Multiple Sclerosis (MS) lesions in multispectral magnetic resonance (MR) imaging. Based on the Fuzzy C-Means (FCM) algorithm, the method starts with a segmentation of an MR image to extract an external CSF/lesions mask, preceded by a local image contrast enhancement procedure. This binary mask is then superimposed on the corresponding data set yielding an image containing only CSF structures and lesions. The FCM is then reapplied to this masked image to obtain a mask of lesions and some undesired substructures which are removed using anatomical knowledge. Any lesion size found to be less than an input bound is eliminated from consideration. Results are presented for test runs of the method on 10 patients. Finally, the potential of the method as well as its limitations are discussed.

Keywords: Magnetic resonance imaging; Multiple Sclerosis; Fuzzy clustering; Segmentation

1. Introduction

Multiple Sclerosis (MS) is the most common nontraumatic disabling neurological disease among young adults. It is a disease of the central nervous system that involves mainly damage

* Corresponding author. Tel.: +33-01-49-40-40-62; fax: +33-01-49-40-33-66.
E-mail address: abdel.boudra@l2ti.univ-paris13.fr (A.-O. Boudraa).

0010-4825/00/$ - see front matter
PII: S0010-4825(99)00019-0

to the myelin sheath that envelops neuronal fibers called axons. Since these axons transmit signals from one part of the body to another, and since this loss of myelin or demyelination results in a disruption of these signals, there is a consequent disruption in body function which relies on the correct transmission of these signals. Demyelination affects essentially the white matter [1,2] of the central nervous system in several discrete areas of various age, size and location. Magnetic resonance (MR) imaging is a very sensitive marker of MS disease [3,4]. It gives a direct insight into the complex histopathology of MS. Demyelination appears as discrete areas of increased signal intensity on proton density (PD) and T_2 weighted images. Because clinical assessment is time consuming, has both low sensitivity and reproducibility, and cannot be blinded, MR imaging is used as a surrogate marker of disease activity. Quantitative assessment of MR imaging lesion load is of great interest in monitoring disease evolution and treatment trial. To this end, image segmentation techniques are required. This operation consists in partitioning (clustering) the MR image into anatomical tissues, fluids and other structures, and assigning anatomically meaningful labels to each component of the image [5]. A commonly used segmentation technique in clinical and research settings is manual tracing [6–8]. This method consists of interactively outlining lesions either on the image or on the zoomed image (up to 4 times magnification) using a mouse or tracker-ball to control a cursor on the computer display. This process is repeated for all slices in which lesions are visible. Although straightforward to implement, manual outlining requires an experienced operator. It is very time consuming and its reproducibility is suboptimal [9]. When dealing with a large number of slices to be processed, automated and semi-automated methods become necessary to save human resources and to avoid intra- and inter-operator variabilities. Different approaches have been proposed for automatic and semi-automatic detection of MS lesions with varying degree of automation and user interaction [10–14,16]. These methods can be categorized into classical, statistical, fuzzy and neural network methods. For example, Broderick et al. [10] used the product and difference of T_2 and PD weighted images as features in combination with thresholding and region growing to extract lesions. Raff and Newman [11] explored the potential of an artificial neural network model as an autoassociative memory to detect lesions. However, to be fully operator independent, multiple processing steps are needed in complete detection procedure. In the semi-automatic method proposed by Johnston et al. [12], a modified version of the Iterated Conditional Modes (ICM) is used to separately segment the PD and T_2 weighted images into tissue probability maps. These maps are then combined and thresholded. A white matter and lesion mask is obtained to which the ICM is again applied to segment lesions. This detection technique requires some a priori knowledge about the various tissues under consideration. Kamber et al. [13] reported a model-based segmentation method. Brain images are mapped to a standard Talairach space and averaged in this space to get probability models for various tissues. The training sets used by this method require selection by the operator of areas of high probability for each tissue type. Raya [14] designed a rule-based segmentation system using two-dimensional (2D) region growing for initial segmentation and confidence functions for combining feature information for vector valued (multiple echo) three-dimensional (3D) MR imaging data sets. Raya derived low-level features enhancing different structures to be identified. The proposed system is very dependent on the imaging protocol used. Udupa and Samarasekera have introduced the concept of fuzzy connectivity [15]. Based on this concept, an MS lesion quantification method is designed. The method is

built on the premise that object information presented in MR images is inherently fuzzy and that local image properties within an object of interest exhibit spatial contiguity, which is also a fuzzy phenomenon [16]. User assistance, in this method, is taken in two steps, first in recognizing major tissues (white matter, gray matter,...) and second in either accepting or rejecting computer detected lesions. In general, the boundaries of real data structures (clusters) are not well defined (fuzzy) in MR imaging data where the transition from one biological tissue to another is not abrupt but smooth. Each pixel or voxel contains more than one tissue type. Thus, an image point belongs to different tissues with varying membership degrees. Fuzzy segmentation techniques have shown promise in segmenting medical images such as in isotopic ventriculography [17,18], positron emission tomography [19] and MR imaging [20–22].

In spite of relatively abundant literature on the processing of MR brain images, the automatic segmentation of MS lesions in MR imaging remains a persistent problem to be resolved. The purpose of this paper is, therefore, to develop a powerful low-level segmentation paradigm, the use of which in combination with some simple knowledge-based rules gives a robust final segmentation of MS lesions in MR images. The low-level segmentation paradigm is essentially based on the use of a Fuzzy C-Means (FCM) clustering algorithm, which is an unsupervized pixel classification technique based on iterative approximation to local minima of global objective function. Applied to the MR images preprocessed using a local image contrast enhancement and a power law point transformation, the FCM works out MS lesions with no false negative lesions and reduced false positive lesions. Furthermore, most of the remaining false positive lesions, subsequently generated by the used segmentation method, can be readily eliminated, as they are contiguous to the intracranial contour of the brain.

2. Method

The method used for MS lesion segmentation is shown in Fig. 1. PD weighted images are first preprocessed using a local histogram equalization procedure followed by a power law point transformation to increase contrast between CSF and lesions. The intracranial contents of the brain are then extracted from the preprocessed images, using a binary mask, such that the segmentation field is narrowed. Thus, the obtained images, denoted by PD_{ET}, are segmented using the FCM algorithm. A binary mask containing lesions and CSF structures is extracted from this first segmentation. This mask has the highest mean intensity value in T_2 weighted images. The obtained mask is superimposed on the corresponding PD weighted images, to which a second fuzzy clustering is applied to extract the lesions. Finally, objects of size less than a predefined threshold are removed.

2.1. MR imaging data

MR brain image data were acquired routinely on a Siemens 1.5 Tesla Magnetom Vision whole body system, following conventional protocols (TR and TE within fixed intervals: $2000 < TR < 3000$, $15 < TE_1 < 30$, $60 < TE_2 < 90$ ms). The T_2 and PD weighted image data came from 10 patients. Each image volume contained 20–25 nonoverlapped slices, depending on the patients. Each slice was collected at 5 mm intervals over the entire brain, and stored as

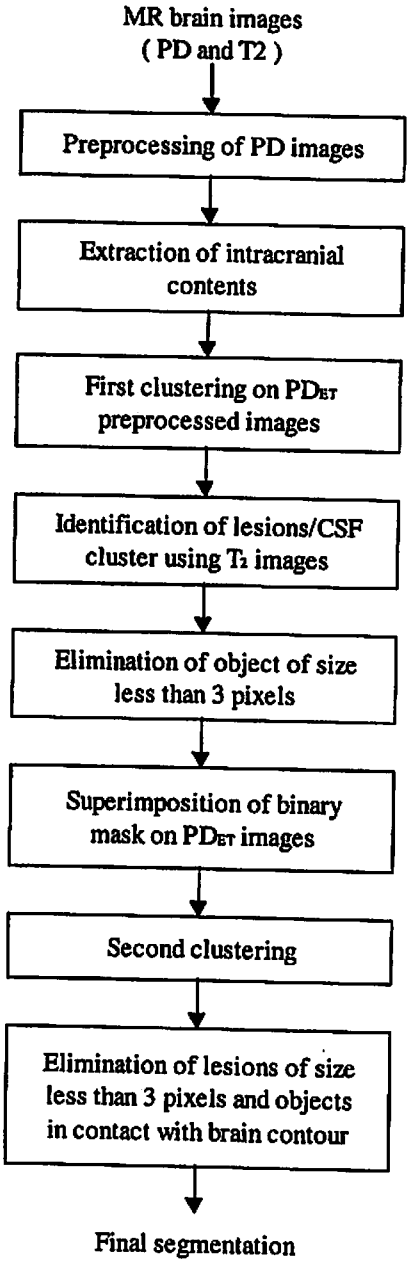

Fig. 1. Block diagram illustrating the MS lesion detection system.

256 × 256 with 1 mm square pixels. Data were transferred via the Internet to a remote Digital DEC 500/400 workstation, on which all computations were done.

2.2. Preprocessing of PD images

Image enhancement process increases the relative intensity level of the wanted structures in the image, and consequently improves their detection sensitivity. Among the existing image enhancement methods, histogram equalization is a simple and robust technique for image contrast enhancement. The possible limitation of histogram enhancement arises where there is a variation in contrast across the image, which is the case for MR brain images. To cope with this problem, histogram equalization is locally applied.

In local histogram equalization, a window W of size $M \times M$ is used. The transformation of the central pixel in the windowed region of the image is found by equalizing the histogram of the windowed region [23]. Let L be the number of discrete gray levels in the image S, i.e., $S(x,y) \in \{0,\ldots, L-1\}$. The discrete density function of the windowed region is given by

$$p_w(l) = \frac{n_l}{M^2} \tag{1}$$

for $l = 0,\ldots, L-1$, where n_l is the number of pixels in the window with gray level l. The distribution function, P_w, of windowed region is given by [24]

$$P_w(l) = 0.5 \times p_w(l) + \sum_{j=0}^{l-1} p_w(j) \tag{2}$$

The histogram equalization transformation, T_{HE}, over the windowed region centered at pixel (x,y) is achieved by

$$T_{HE}(S(x, y)) = (L-1) \times P_w(S(x, y)) \tag{3}$$

This operation increases the contrast of lesions having weak gray levels and shifts the lesion intensity values to extreme values of the histogram dynamic range.

After local histogram equalization, all objects presenting greater gray levels in the image have been enhanced. In order to bring out only lesions, the following transformation is performed.

$$G(x, y) = [S(x, y)]^p \tag{4}$$

It maps each pixel $S(x,y)$ to its pth power $G(x,y)$. The appropriate choice of p allows the intensity difference between lesions and CSF structures to be amplified.

2.3. Extraction of intracranial contents

Before applying FCM clustering process, tissues surrounding brain are discarded. Thus, pixels lying outside the brain contour and which are not of interest (skin, fat, bone and air) can be eliminated. Furthermore, these pixels share intensity with the structures of interest that

we are attempting to extract. By limiting the segmentation to brain, the computation time is largely reduced. The intracranial cavity was automatically detected using a technique developed in our laboratory. The method is a 2D multiresolution algorithm using pyramidal data structures [25].

2.4. Fuzzy segmentation method

Let $X=\{x_1,\ldots,x_n\}$ be a finite data set and $c\geqslant 2$ an integer; and let $R^{c\times n}$ denote the set of all real $c \times n$ matrices. A fuzzy c-partition of X is represented by a matrix $U=[\mu_{ik}] \in R^{c\times n}$, the entries of which satisfy

$$\mu_{ik} \in [0,\ 1]\ 1\leqslant i\leqslant c;\ 1\leqslant k\leqslant n$$

$$\sum_{i=1}^{c}\mu_{ik}=1;1\leqslant k\leqslant n$$

$$\sum_{k=1}^{n}\mu_{ik}>0;1\leqslant i\leqslant c \tag{5}$$

U can be used to describe the cluster structure of X by interpreting μ_{ik} as the degree of membership of x_k to cluster i. Good partitions U of X may be defined by the minimization of the fuzzy c-means objective functional [26]:

$$J_m(U,\ V{:}X)=\sum_{k=1}^{n}\sum_{i=1}^{c}(\mu_{ik})^m\|x_k-v_i\|_A^2 \tag{6}$$

where $m\in[1,\ +\infty]$ is a weighting exponent called the fuzzifier, $V=(v_1,v_2,\ldots,v_c)$ is the vector of the cluster centers. $\|\ x\ \|_A=\sqrt{x^TAx}$ is any inner product norm where A is any positive definite matrix. Approximate optimization of J_m by the FCM algorithm is based on iteration through the following necessary conditions for its local extrema:

FCM Theorem ([26]). Assume $m\geqslant 1$ and $\|x_k-v_i\|_A^2>0$, $1\leqslant i\leqslant c$, $1\leqslant k\leqslant n$. (U,V) may minimize J_m only if:

$$\mu_{ik}=\left[\sum_{j=1}^{c}\left(\frac{\|x_k-v_i\|_A}{\|x_k-v_j\|_A}\right)^{\frac{2}{(m-1)}}\right]^{-1} \tag{7}$$

$$v_i=\frac{\sum_{k=1}^{n}(\mu_{ik})^m\cdot x_k}{\sum_{k=1}^{n}(\mu_{ik})^m} \tag{8}$$

The FCM algorithm consists of iterations alternating between Eqs. (7) and (8). This algorithm converges to either a local minimum or a saddle point of J_m [26]. Recently, a fast version of the FCM was proposed in [27]. The proposed algorithm is based on one dimensional attribute such as the gray-level. Let H be the histogram of image of L-levels, where L is the number of gray levels. Each pixel has a feature that lies in the discrete set $X=\{0,1,\ldots,L-1\}$.

In the new formulation, FCM minimizes the following functional, which is very similar to that of [26]:

$$J_m(U, V{:}L) = \sum_{l=0}^{L-1}\sum_{i=1}^{c}(\mu_{il})^m \cdot H(l) \cdot \|l - v_i\|_A^2 \tag{9}$$

The FCM only operates on the histogram and hence is faster than the conventional version which processes the whole data set. Thus, the computation of the membership degrees of $H(l)$ pixels is reduced to that of only one pixel with l as gray level value. The algorithm is outlined in the following steps:

⟨FCM1⟩ Fix the number of clusters c, $2 \leqslant c \leqslant L$, and the threshold value ϵ.

⟨FCM2⟩ Find the number of occurrences, $H(l)$, of the level l; $l = 0,1,2,\ldots,L-1$.

⟨FCM3⟩ Initialize the membership degrees μ_{il} using the L gray levels such that:

$$\sum_{i=1}^{c}\mu_{il} = 1;\ l = 0,\ 1,\ \ldots,\ L-1$$

⟨FCM4⟩ Compute the centroid v_i as follows:

$$v_i = \frac{\sum_{l=0}^{L-1}(\mu_{il})^m \cdot H(l) \cdot l}{\sum_{l=0}^{L-1}(\mu_{il})^m \cdot H(l)} \quad i = 1,\ \ldots,\ c$$

⟨FCM5⟩ Update the membership degrees

$$\tilde{\mu}_{il} = \left[\sum_{j=1}^{c}\left(\frac{\|l - v_i\|_A}{\|l - v_j\|_A}\right)^{\frac{2}{(m-1)}}\right]^{-1}$$

⟨FCM6⟩ Compute the defect measure

$$E = \sum_{i=1}^{c}\sum_{l=0}^{L-1}|\tilde{\mu}_{il} - \mu_{il}|$$

If $(E > \epsilon)\{$
$\mu_{il} \leftarrow \tilde{\mu}_{il}$
goto ⟨FCM4⟩$\}$

⟨FCM7⟩ Defuzzification process

2.5. Connected components

A connected component is a maximal set of connected pixels sharing the same label. Connectivity can be defined in terms of their adjacency. The connectivity is a very interesting topological attribute for extraction of regions of interest.

Let π be a bounded subset of an image indexed by (i,j), and $P(i_P,j_P)$ and $Q(i_Q,j_Q)$ two 1-valued image points. $P(i_P,j_P)$ is associated to the following subsets:

$$N_1(P) = \{Q \in \pi; d_1(P, Q) \leqslant 1\}$$

$$N_2(P) = \{Q \in \pi; d_2(P, Q) \leqslant 1\}$$

where d_1 and d_2 are the metrics defined by the following relations:

$$d_1(P, Q) = |i_P - i_Q| + |j_P - j_Q|$$

$$d_2(P, Q) = \max(|i_P - i_Q|, |j_P - j_Q|)$$

Two arbitrary points P and Q are 8-neighbors if $d_2(P,Q) \leqslant 1$ and 4-neighbors if $d_1(P,Q) \leqslant 1$. The pixels (i_1,j_1) and (i_k,j_k) are said to be connected by an 8-path (4-path) if there exists a sequence of 1-valued pixels (i_m,j_m), $2 \leqslant m \leqslant k$, such that each pair of pixels (i_{m-1},j_{m-1}) and (i_m,j_m) are 8-neighbors (4-neighbors). The subsets $N_1(P)$ and $N_2(P)$, containing P, are called the 8-*neighborhood* and 4-*neighborhood* of the point P. To separate different connected components, a labeling technique is used.

2.6. Labeling

Labeling the connected regions of an image is a fundamental problem in image processing and machine vision. The labeling process consists in assigning a unique label to each connected component in the image. Thus, two 1-valued points share the same label if and only if they are in the same connected component. The labeling algorithm used consists in assigning a label to the connected components of a given class, and in propagating this label locally among adjacent pixels of each component to obtain an identical label for all pixels of the same component.

To label a connected region S, the corresponding cluster is associated to d_1-connected component (the extension to d_2-connectivity is obvious). The following is the major steps of the labeling algorithm.

/*Initialization*/

Step (1)

$k \leftarrow 0$;
for $j = 1,\ldots,M$
  for $i = 1,\ldots,M$

$IC^k(i,j) \leftarrow M*M + 1;$
if $(IC(i,j)=1)$ $IC^k(i,j) \leftarrow (i-1)*M+j;$

/*Label propagation*/

Step (2)

$k \leftarrow k + 1;$
for $j = 2,\ldots,M$
  for $i = 2,\ldots,M$
    $IC^{k+1}(i,j) \leftarrow \min(IC^k(i,j),IC^k(i-1,j),IC^k(i+1,j),IC^k(i,j-1),IC^k(i,j+1));$
    if $(IC^k(i,j)=M*M+1)IC^{k+1}(i,j) \leftarrow IC^k(i,j);$

Step (3)

for $j = 2,\ldots,M$
for $i = 2,\ldots,M$
  if $(IC^{k+1}(i,j) \neq IC^{k+1}(i,j))$ goto Step 2;

where $IC()$ is the binary image containing the cluster that we want to separate from its different connected components. At the initialization, a label is assigned to each S element corresponding to its position in image $IC()$.

2.7. Quantitative analysis

To quantify the performance of the segmentation results obtained by the proposed method, in comparison with those given by trained human experts (radiologist and neurologist), two similarity indices are evaluated:

$$SI_1 = \frac{|A \cap M|}{|M|}$$

$$SI_2 = \frac{N_{obj}(A \cap M)}{N_{obj}(M)}$$

A (automatic) and M (manual) are binary objects in the two segmentation images to be compared. $N_{obj}(F)$ is the number of objects in a set F. These indices are symmetric in A and M, and take values in the interval [0,1]. SI_1 and SI_2 allow to estimate the rate of false negatives in terms of areas and number of lesions, respectively. When $SI_1 = SI_2 = 0$, the automatic and manual masks are completely disjointed. The similarity index $SI_1 = 1$ means that the automatic and manual segmentations give the same areas. The similarity indice $SI_2 = 1$ indicates that no lesions are missed. Experts manually segment the slice by outlining what they

perceived and estimated as the contours of lesions. T_2 and PD images are displayed to facilitate visualization.

3. Results

Quantitation based on T_2 and PD weighted images is currently considered to be the primary image-based marker of MS lesions [16]. These two images are strongly correlated (and also spatially registered), and show the lesions as hypersignal regions.

The detection method is run in 10 patients. In Fig. 2a and b an example of PD and T_2 weighted images are shown in patient with MS lesions. One may note that the lesions appear as brighter objects. This characteristic of MS lesions in PD images was made more visible after a local histogram equalization as seen in Fig. 2c. Note that this operation has also increased the separability between lesions and the remaining brain structures. The local histogram equalization was obtained using a window of size 50 × 50. The final preprocessing result, obtained by applying the power law point transformation, is illustrated in Fig. 2d, in which each pixel was mapped to its square value. Using the binary mask (Fig. 2e) given by the procedure described in [25], the generated noise, outside the brain space, is easily eliminated (Fig. 2f). The fuzzy segmentation of PD_{ET} image, illustrated in Fig. 2f, is performed using $c = 3$ and $\epsilon = 10^{-3}$. The result is shown in Fig. 3a. For each cluster the corresponding T_2 intensity mean value is calculated and the highest one corresponds to the CSF spaces/lesions binary mask (Fig. 3b). This is because the CSF spaces (ventricles and sulci) and lesions are bright on the T_2 weighted image. One may remark that all the lesions and structures within the same intensity range as lesions are in the same cluster (Fig. 3b). The binary mask (Fig. 3b) is superimposed on the corresponding PD_{ET} image where a second segmentation is performed with $c = 2$, $\epsilon = 10^{-3}$. This segmentation (Fig. 4a), compared to the first one (Fig. 3a), conserves all regions of interest and undesirable structures are reduced. As in the first step (Fig. 3b), a second binary mask (Fig. 4b) is extracted from the segmented image (Fig. 4a) using T_2 information. The labeling result of the connected components of the mask (Fig. 4b) is shown in Fig. 5a. Based on anatomical knowledge, objects of size less than 3 pixels and those in contact with brain contour are eliminated. The final result is shown in Fig. 5b.

To show the performance of the proposed method, we give in Table 1, the similarity indices calculated for the entire set (all slices) of MR images in one patient. In Table 2 are reported the similarity indices values for three representative levels of brain with varying degree of segmentation difficulty.

The results comparison in 10 patients of the manual and automated methods are reported in Tables 1 and 2. SI_2 values listed in Table 1 show that there is a good overlap ($SI_2 = 0.87$), in terms of number of detected lesions, between the segmentation methods except for slices 17–18. These values suggest that there are a few false negatives. These findings are confirmed by the results obtained in 10 patients (Table 2). On the other hand, the SI_1 values indicate that there is a relatively good agreement between the two methods ($SI_1 = 0.65$) (Table 1). A careful examination of Table 2 shows that SI_1 values are only smaller in the bottom slices of the brain.

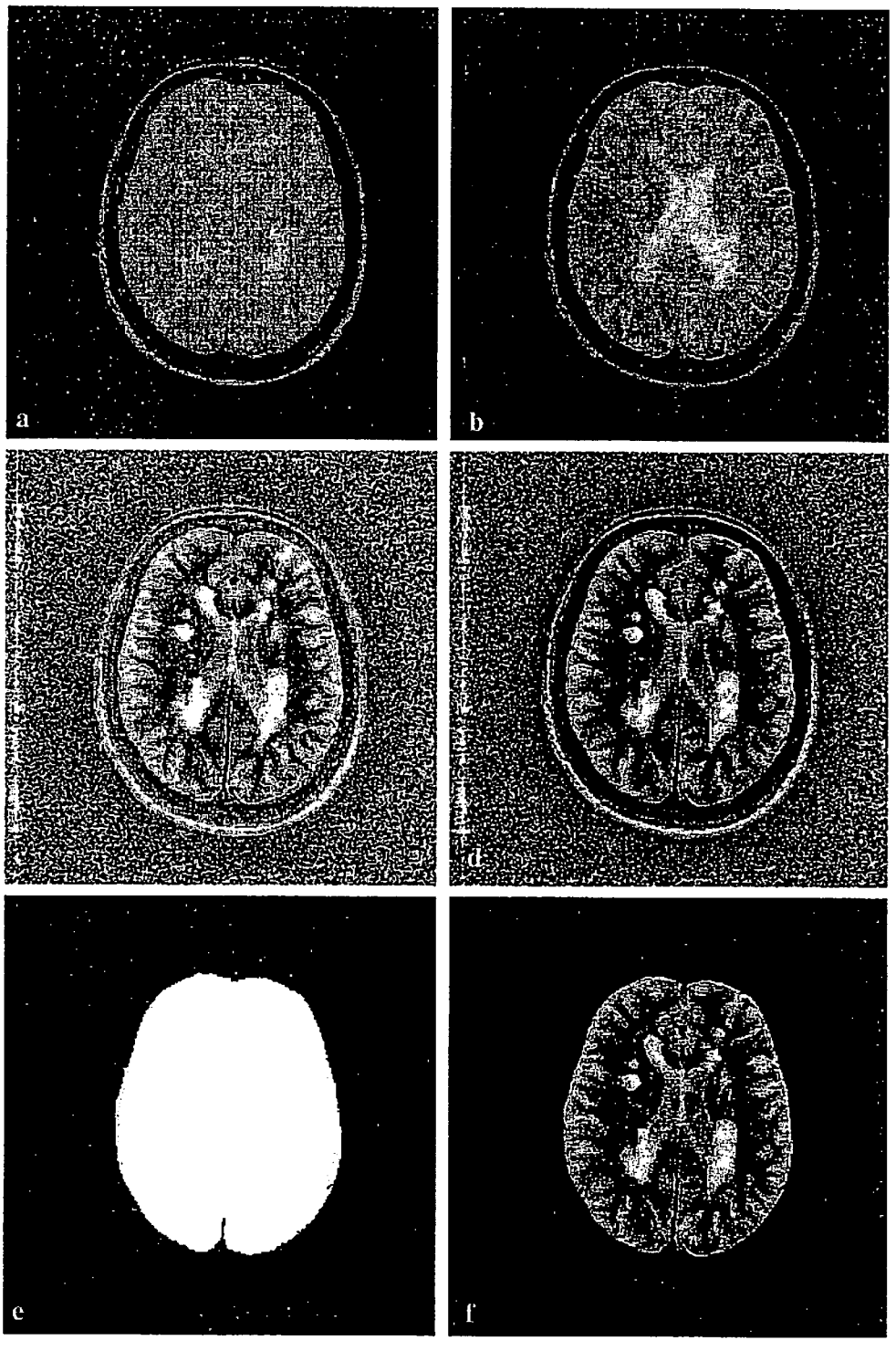

Fig. 2. Local contrast enhancement preprocessing. (a) Original PD weighted image. (b) T_2 weighted image. (c) Local histogram equalization result. (d) Power law point transformation result ($p = 2$). (e) Binary mask of intracranial region. (f) Extraction of the intracranial contents.

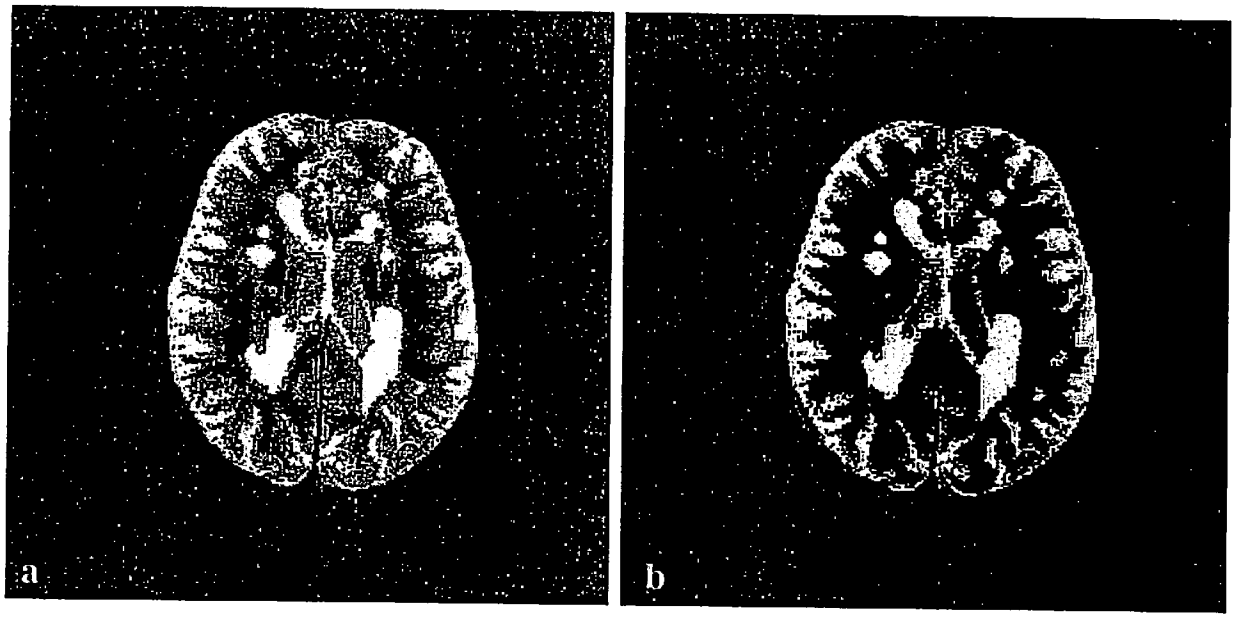

Fig. 3. First fuzzy segmentation. (a) Segmentation with three clusters of the preprocessed PD image obtained in Fig. 2d. (b) Extracted binary mask (CSF spaces/lesions) using information from T_2.

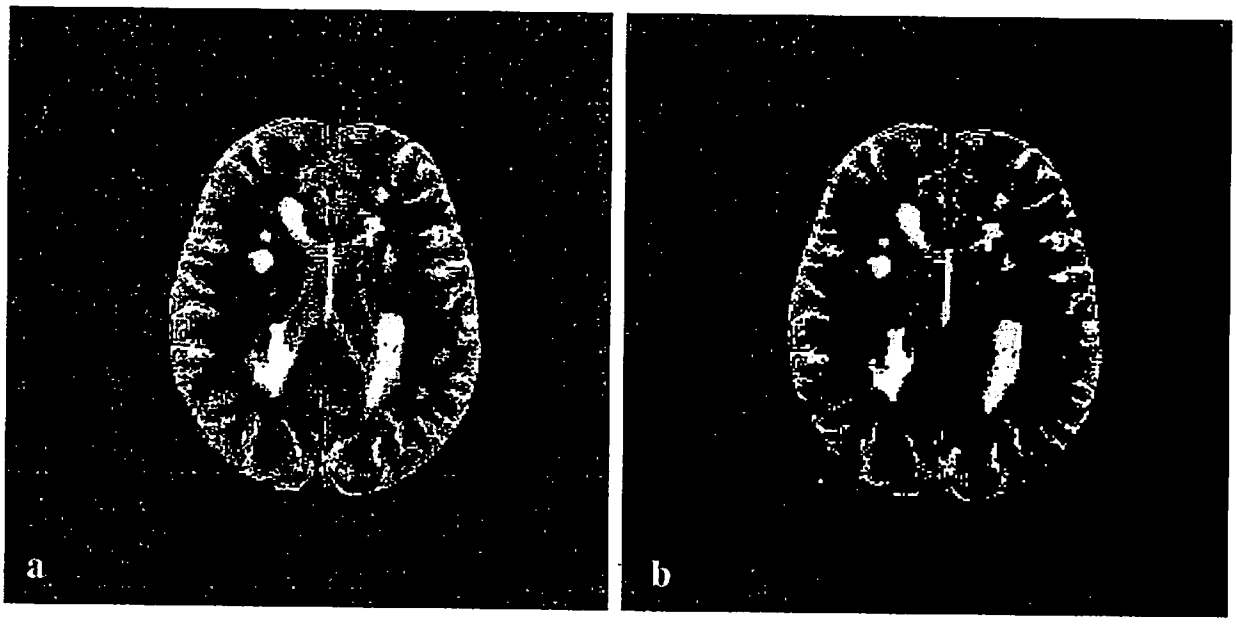

Fig. 4. Second fuzzy segmentation. (a) Segmentation with three clusters of PD image masked by the cluster obtained in Fig. 3b. (b) Extracted binary mask (CSF spaces/lesions) using T_2 information.

Fig. 5. Image postprocessing. (a) Labeling result of the connected components of binary mask. (b) Final result obtained using anatomical knowledges.

4. Discussion

The goal of this study was to develop a robust low-level image-processing method for segmentation of MS lesions. A fully automated lesion extraction is reliable, eliminates intra- and inter-observer variabilities and is reproducible. Fuzzy clustering has shown promise in segmentation of MR images.

Before segmentation, a local image enhancement process is performed. The aim of this preprocessing step is to improve the lesion contrast and thus to convert the PD image to a form better suited for segmentation. This processing ensures that all regions of interest (lesions) remain in the same cluster. Different window sizes (W) ranging from 10 to 70 are tested to locally enhance the PD image. Indeed, there is no method to automatically find the adequate window size. It is difficult to know a priori where the contrast needs to be enhanced and the required degree of enhancement. The processing of a large number of PD images (10 patients, each with 22 slices) has shown that more accurate results (homogeneous appearance of lesions) are obtained with $W = 51$. Although small windows ($W < 51$) improve contrast of some lesions, the contrast is dramatically degraded for large lesions. The enhancement increases the heterogeneity of these large lesions. We have also observed that for $W > 51$ the contrast is not more improved than with $W = 51$. However, for all sizes used, it is impossible to boost the signal without enhancing noise. The enhancement of noise is especially visible in relatively uniform regions of the image. This is the case of the external brain region (image background) (Fig. 2c). Thus, in limiting segmentation to brain region using detection procedure of intracranial region (Fig. 2f), this region of artifacts is avoided. The main drawback in using local enhancement is that undesired structures that fall within the same intensity as lesions, such as external CSF or eyes, are also enhanced and this creates additional false positives.

Table 1
Similarity indices for each slice in one patient

Slice	SI_1	SI_2
1	0.54	1.00
2	0.45	0.70
3	0.52	0.78
4	0.67	0.89
5	0.77	1.00
6	0.78	1.00
7	0.86	1.00
8	0.73	0.71
9	0.67	0.93
10	0.78	0.89
11	0.65	0.92
12	0.75	0.80
13	0.84	0.71
14	0.62	1.00
15	0.69	1.00
16	0.64	0.80
17	0.52	0.40
18	0.64	0.50
19	0.69	1.00
20	0.20	1.00
21	0.68	1.00
22	0.60	1.00
Mean	0.65	0.87

Table 2
Similarity indices for three slices (top, middle, bottom) in nine patients

	Top slice		Middle slice		Bottom slice	
Patients	SI_1	SI_2	SI_1	SI_2	SI_1	SI_2
1	0.45	0.70	0.65	0.92	0.68	1.00
2	0.48	0.75	0.72	0.90	0.50	1.00
3	0.57	0.50	0.44	0.78	0.29	0.50
4	1.00	1.00	0.87	0.90	0.86	0.80
5	0.56	1.00	0.64	0.64	0.56	1.00
6	0.93	1.00	0.86	1.00	0.46	0.50
7	0.80	0.83	0.89	1.00	0.51	0.83
8	0.46	0.91	0.60	0.83	0.31	0.67
9	0.87	1.00	0.71	1.00	0.50	1.00
10	0.51	0.90	0.51	0.82	0.31	0.67
Mean	0.66	0.86	0.69	0.88	0.50	0.80

The best result of power law point transformation is obtained using $p = 2$. For this value, the transformation is piecewise linear for the intensity interval corresponding to the lesions. However, for $p \geqslant 3$ the corresponding transformation led to splitting of the lesion region into several components with varying contrasts. Consequently, some components are assigned to different tissue types. This complicates the lesion tracking and also produces false negatives. This effect is expected since, in general, large lesions present a given heterogeneity. These gray scale inhomogeneities become more apparent for lesions of large area. Thus, in this case and using $p \geqslant 3$, the differences between lesion pixels are largely stretched.

Each preprocessed image is first segmented into three classes: white matter, gray matter and CSF (i.e., $c = 3$). The number of classes c is set to 3 to avoid splitting of lesions in more than one cluster. This is the case for $c > 3$. This first segmentation may be viewed as a coarse one. However, in setting c to 3 and using the FCM we do not claim to segment brain in three pure tissues. Our aim, in this first step, is only to track lesions and keep them in the same cluster. Since lesions and CSF are the brightest structures of the brain on T_2 weighted images, the mean value of the CSF/lesions mask is the highest one. This valuable piece of information is used to identify the CSF/lesions cluster. The coarse step yields a mask which contains all information of interest for the fine step but with many false positives. The FCM is then reapplied to the image masked on the preprocessed PD image using $c = 2$. The second processing allows, essentially, to refine the results of the first step and in particular to extract lesions connected to the sulci. Thus, in postprocessing, elimination of sulci is done without affecting lesions. As another postprocessing, a lesion of size less than 3 pixels is removed. However, in spite of the postprocessing used, a number of false positives remain. Consequently, more sophisticated rules may be incorporated to complete elimination of false positives. These rules may be given by experts and translated and coded as "if–then" fuzzy rules.

The proposed method does not generate false negatives in the central region of the brain and especially in the periventricular region. However, false negatives may occur near the brain contour. This is due to the brain isolation procedure which produces, in certain cases, unreliable contours. In other words, certain lesions could be excluded by postprocessing and not by the FCM algorithm. Fortunately, in general, lesions do not often occur near the brain contour.

The SI_2 values listed in Tables 1 and 2 show the good agreement between the proposed method and the manual one. These values clearly show that the number of false negatives is largely reduced. These results are made possible due to the incorporation of the preprocessing step that provided increased contrast between the lesions and the brain tissues and facilitated the segmentation process. It is important to keep in mind that the manual method is considered as the gold standard method. Establishment of accuracy in segmentation is an elusive phenomenon since truth is unknown [16]. Even with this good agreement, the false positives arise because of the confusion of lesions with gray matter. This is due in part to the difficulty in isolating pure tissues in such thick slices (5 mm thick), to the residual RF inhomogeneity which has not been corrected in the present study. The SI_1 values indicate that there is a fairly good overlap between the automated and manual segmentation methods. We have noticed that lesion areas are relatively smaller than those found by the operator. Human operator tends to draw boundaries well around ROI's whereas automatic methods tend to

yield more conservative measures. Due to the partial volume effect, the edges of the tissues or lesions are not well defined and consequently their perception and their correct delineation are not easy. This difficulty becomes more important when the operator delineates small lesions or irregularly shaped ones. Therefore, the correction of the partial volume effect is necessary. Since we are mainly interested in MR imaging follow up of MS patients, it is more important to have good reproducibility rather than to have either false positives or false negatives.

5. Summary

A fully automated method for MS lesion segmentation is proposed. Acceptable segmentation of the lesions are obtained in 10 patients without any human intervention. There is a good agreement with lesions outlined manually by the experts. Future work will include improving the preprocessing steps such as RF inhomogeneity and partial volume effect corrections. More sophisticated postprocessing is envisaged to reduce the false positives. Finally, we plan to investigate the three-dimensional extension of the proposed method in order to measure more precisely the lesion volume.

References

[1] K.R. Marvilla, Multiple sclerosis, in: D.D. Stark, W.G. Bradely (Eds.), Magnetic resonance imaging, Mosby, St Louis, MO, 1988, pp. 344–358.
[2] R. Grossman, D. Tousem, White matter diseases, in: J. Thrall (Ed.), Neuroradiology: The Requisities, Mosby, St Louis, MO, 1994, pp. 201–224.
[3] R.I. Young, A.S. Hall, C.A. Pallis, et al., Nuclear magnetic resonance imaging of the brain in multiple sclerosis, Lancet 2 (1981) 1063–1066.
[4] R. Grossman, S. Gonzalez, S. Atlas, et al., Multiple sclerosis: gadolinium enhancement in magnetic resonance imaging, Radiology 161 (1986) 721–725.
[5] A. Lundervold, G. Stovik, Segmentation of brain parenchyma and cerebrospinal fluid in multispectral MR images, IEEE Trans. Med. Imag. 14 (1995) 339–349.
[6] P. Maeder, A. Virsen, M. Bajc, et al., Volumes of chronis traumatic frontal brain lesions measured by MR imaging and CBF tomography, Radiology 32 (1991) 271–278.
[7] D. Paty, D. Li, J. Oger, L. Kastrukoff, R. Koopmans, E. Tanton, G.J. Zhao, Magnetic resonance imaging in the evaluation of clinical trials in multiple sclerosis, Ann. Neurol. 36 (1994) 95–96.
[8] F. Lublin, R. Krober, S. Ehrlich, Distributional patterns of multiple sclerosis brain lesions, J. Neuroimag. 4 (1994) 188–195.
[9] J. Grimaud, M. Lai, J. Thorpe, P. Adeleine, L. Wang, G.J. Barker, D.L. Plummer, P.S. Tofts, W.I. McDonald, D.H. Miller, Quantification of MRI lesion load in multiple sclerosis: a comparison of three computer-assisted techniques, Magn. Res. Med. 4 (1996) 495–505.
[10] J. Broderick, S. Narayan, M. Gaskill, A. Dhawan, J. Khoury, Volumetric measurement of multifocal brain lesions, J. Neuroimag. 6 (1996) 36–43.
[11] U. Raff, F.D. Newman, Automated lesion detection and lesion quantitation in MR images using autoassociative memory, Med. Phys. 19 (1991) 71–77.
[12] B. Johnston, M.S. Atkins, B. Mackiewich, M. Anderson, Segmentation of multiple sclerosis lesions in intensity corrected multispectral MRI, IEEE Trans. Med. Imag. 15 (1996) 154–169.
[13] M. Kamber, R. Shinghal, D.L. Collins, S.F. Gordon, A.C. Evans, Model-based 3D segmentation of multiple sclerosis lesions in Magnetic Resonance brain images, IEEE Trans. Med. Imag. 14 (1995) 442–453.

[14] S.P. Raya, Low-level segmentation of 3D Magnetic Resonance brain images: A rule-based system, IEEE Trans. Med. Imag. 9 (1990) 327–337.
[15] J.K. Udupa, S. Samarasekera, Fuzzy connectedness and object definition: Theory, algorithms and application in image segmentation, Graphical Models Image Processing 58 (1996) 246–261.
[16] J.K. Udupa, L. Wei, S. Samarasekera, Y. Miki, M.A. Van Buchem, R.I. Grossman, Multiple sclerosis lesion quantification using fuzzy-connectedness principles, IEEE Trans. Med. Imag. 16 (1997) 598–609.
[17] A.E. Boudraa, J.J. Mallet, J.E. Besson, S.E. Bouyoucef, J. Champier, Left ventricle automated detection method in gated isotopic ventriculography using fuzzy clustering, IEEE Trans. Med. Imag. 12 (1993) 451–465.
[18] A.E. Boudraa, M. Arzi, J. Sau, Marinier D. Sappey, J.J. Mallet, Automated detection of the left ventricular region in gated nuclear cardiac imaging, IEEE Trans. Biomed. Eng. 43 (1996) 430–437.
[19] A.E. Boudraa, J. Champier, L. Cinotti, J.C. Bordet, F. Lavenne, J.J. Mallet, Delineation and quantitation of brain lesions by fuzzy clustering in positron emission tomography, Comput. Med. Imag. Graph. 20 (1996) 31–41.
[20] A.E. Boudraa, Automated detection of the left ventricular region in magnetic resonance images by fuzzy c-means model, Int. J. Cardiac Imag. 13 (1997) 349–357.
[21] A.E. Boudraa, Image Fuzzy Segmentation: Application to Isotopic Ventriculography, Magnetic Resonance Imaging and Positron Emission Tomography. PhD Thesis, University of Lyon, 1994.
[22] J.C. Bezdek, L.O. Hall, L.P. Clarke, Review of MR images segmentation techniques using pattern recognition, Med. Phys. 20 (1993) 1033–1048.
[23] R. Dale-Jones, A. Tjahjadi, A study and modification of the local histogram equalization algorithm, Pattern Recognition 26 (1993) 1373–1381.
[24] R.A. Hummel, Histogram modification techniques, Computer Graphics Image Processing 4 (1975) 209–224.
[25] P. Pachai. Automated segmentation and quantification of MS lesions in MRI, MSc. National Institute of Applied Sciences of Lyon, France. 1996.
[26] J.C. Bezdek, Pattern Recognition with Fuzzy Objective Function Algorithms, Plenum Press, New York, 1981.
[27] A.E. Boudraa, P. Clarysse, Fast fuzzy gray level image segmentation method, Medical Biological Engineering Computing 35 (1997) 686.

Abdel-Ouahab Boudraa graduated from the Institute of Physics, Constantine University, Algeria, in 1987. He received a University degree in Nuclear Magnetic Resonance in 1993, a PhD degree in Biomedical Engineering in 1994 and University degrees in Statistics and Modeling in 1995 and Positron Emission Tomography in 1997 all from the University of Claude Bernard, Lyon 1, France. In 1998, he joined the University Paris 13 (Institut Galilée) where he is currently an associate professor of Electrical Engineering. His current research interests include computer vision, vector quantization, data structures and analysis, hard and fuzzy pattern recognition and applications of fuzzy set theory to medical image. Dr. Boudraa is an Associate Member of IEEE Society.

Sidi Mohammed Réda Dehak received the MS degree in Signal and Image processing in 1998 from National Institute of Applied Sciences (INSA), Lyon, France and the Engineer degree in Computer Science in 1997 from University of Sciences and Technology, Oran, Algeria. He is currently working towards his PhD degree in Signal and Image processing at ENST of Paris, France. His research interests include Approximate Reasoning, Spatial Relationship and Fuzzy sets Theory.

Yue-Min Zhu received a BS degree in electrical engineering from Huazhong University of Science and Technology, Wuhan, China, in 1982. He obtained an MS degree (1984) and a Ph.D. (1988) from the INSA (Institut National des Sciences Appliquées) of Lyon, France. He also obtained the "Habilitation à Diriger des Recherches" in 1993. He is a permanent researcher of the CNRS (Centre National de la Recherche Scientifique). His current research projects are MR image segmentation, ultrasonic and x-ray image fusion, and high resolution x-ray imaging systems. His research interests include time-frequency analysis, multiresolution analysis, local spectral analysis, image segmentation, data fusion and real-time x-ray imaging.

Chahin Pachai obtained an Electrical and Electronic Engineering degree (1995) and MS degree in Signal and Image processing (1996) from National Institute of Applied Sciences (INSA), Lyon, France. He is now a PhD student with major focus on various aspects of automatic segmentation of Magnetic Resonance images of human brain.

Yong-Gang Bao is vice professor of the Computer Engineering Department of Changchun University, China. His research interests include distributed database and computer network.

Jérôme Grimaud, MD, is a neurologist from the Claude-Bernard University, Lyon, France, working at the department of Neurology, Hôpital de l'Antiquaille, Lyon, France. He is a member of the European Magnetic Resonance Network in Multiple Sclerosis (MAGNIMS). His research interests include the MRI findings in multiple sclerosis, in terms of sensitivity and specificity.